

MSE-422 - Advanced Metallurgy**Exam 27/01/2023****09h15 – 10h45**

Family name: _____

First name: _____

No. Sciper: _____

| Question | Points |
|---------------|------------|
| 1 | /19 |
| 2 | /20 |
| 3 | /16 |
| 4 | /20 |
| Total: | /75 |
| Grade: | |

- Do not write more text than is necessary; sometimes, you can answer the questions with 1-2 words.
- You can also write on the backside of the sheets. If you do so, please indicate clearly to which question your answer belongs.
- If you need more paper for your answers, please ask.

1) Advanced steels & steel metallurgy (19P)

a) In the table below, several steels are listed with their EN steel name designation. Complete the table by adding the amount of each alloying element in wt.%

Table 1: Designations and compositions of four different steels;

| Nr | Steel | Cr | Ni | Mo | Mn | V | C | N |
|----|----------------------|------|----|----|----|---|------|---|
| 1 | X90CrMoV 18-1-1 | 18 | | 1 | | | 0.9 | |
| 2 | X13CrMnMoN 18-14-3-1 | 18 | | 3 | 14 | | 0.13 | 1 |
| 3 | X3CrNiMo 25-7-4 | 25 | 7 | 4 | | | 0.03 | |
| 4 | 10CrMo9-10 | 2.25 | | 1 | | | 0.1 | |

b) With the help of the Schaeffler diagram below, determine the phases that can be found in each steel.

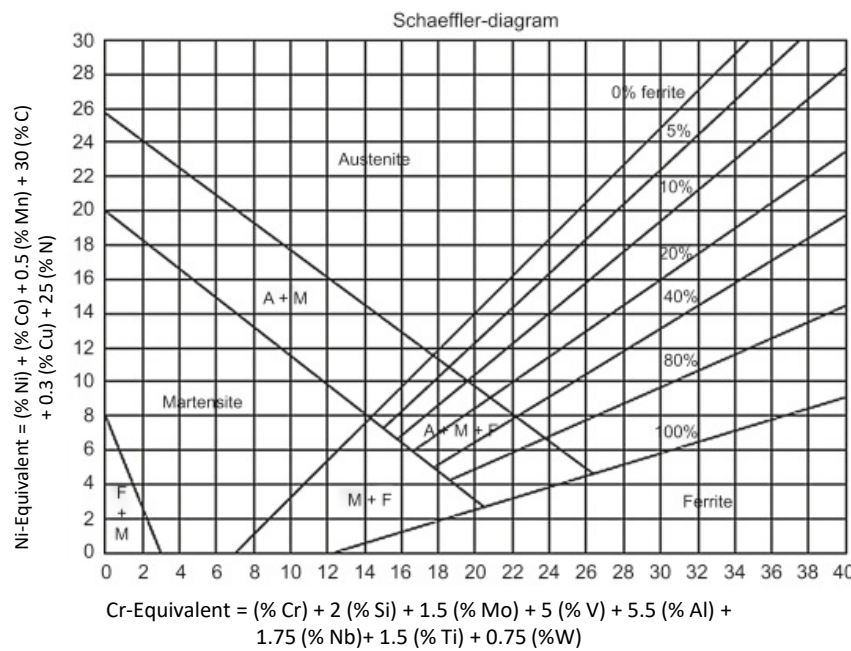


Figure 1: Schaeffler diagram;

Table 2: Designations and phases of four different steels;

| Nr | Steel | Phases |
|----|----------------------|-------------------------------|
| 1 | X90CrMoV 18-1-1 | Austenite |
| 2 | X13CrMnMoN 18-14-3-1 | Austenite |
| 3 | X3CrNiMo 25-7-4 | Ferrite (90%)-Austenite (10%) |
| 4 | 10CrMo9-10 | Martensite |

c) Besides their role as ferrite stabilizers, briefly explain the general role of Cr and Mo in the above mentioned steels.

Mo

- + solid solution strengthener
- + carbide former
- + supports martensite formation
- supports σ -phase formation

Cr

- + carbide former
- supports σ -phase formation

d) Which of the above mentioned steels would you use for the following applications? Justify your answer briefly.

- Sushi knife blades

- Alloy 1:
- Very high amount of C \rightarrow carbide former and formation of martensite
- High amount of Cr \rightarrow good corrosion resistance

- Temporary orthopedic implant for bone fixation

- Alloy 2:
- Austenitic \rightarrow good ductility
- High amount of Cr \rightarrow good corrosion resistance

Alloy 3 also possible: high Cr content \rightarrow good corrosion resistance

e) Boiler tubes for a steam power plant, which are fabricated from the steel 10CrMo9-10, is subjected to the heat treatment steps given below. After the heat treatment a yield strength of 320 MPa, a tensile strength of 580 MPa and an elongation at fracture of 20% are measured.

Heat treatment

- Heating to 970°C and holding for 30 minutes
- Cooling to room temperature in 10 minutes
- Re-heating to 650°C and holding for 120 minutes
- Explain briefly the function of each heat treatment step.
 - Heating → austenite / homogenize (solution treatment)
 - Cooling → martensite: high strength and hardness (quenching)
 - Re-heating → residual stress relief + carbide formation (tempering)

- How would the mechanical properties change (qualitatively) if the final re-heating step would be omitted?
 - More brittle
 - Lower strength (no carbides)
- How would the same three-step heat treatment affect (qualitatively) the mechanical properties of the steel X13CrMnMoN 18-14-3-1? The initial values for the yield strength, tensile strength and elongation at fracture are 460 MPa, 750 MPa and 30%, respectively.
 - The properties would not change. The steel is austenitic and it will stay austenitic also after the heat treatment.

f) Two steels with the compositions given in Table 3, were uniaxially deformed during tensile test until failure.

Table 3: Compositions of the two steels:

| Steel | C | Si | Mn | P | Ni | Cr | Cu | N |
|---------|------|------|-------|-------|------|-------|------|------|
| Steel 1 | 0.15 | 0.45 | 11.09 | 0.041 | 1.97 | 13.36 | 0.04 | 0.18 |
| Steel 2 | 0.08 | 0.47 | 11.04 | 0.042 | 1.18 | 15.93 | 0.03 | 0.2 |

The amount of martensite was measured during the tensile test at different strain levels and the values are plotted in Figure 2-a as a function of the applied strain. It can be seen that the amount of martensite is significantly higher in steel 2 than in steel 1. Figure 2-b shows the stress-strain curves for the two steels.

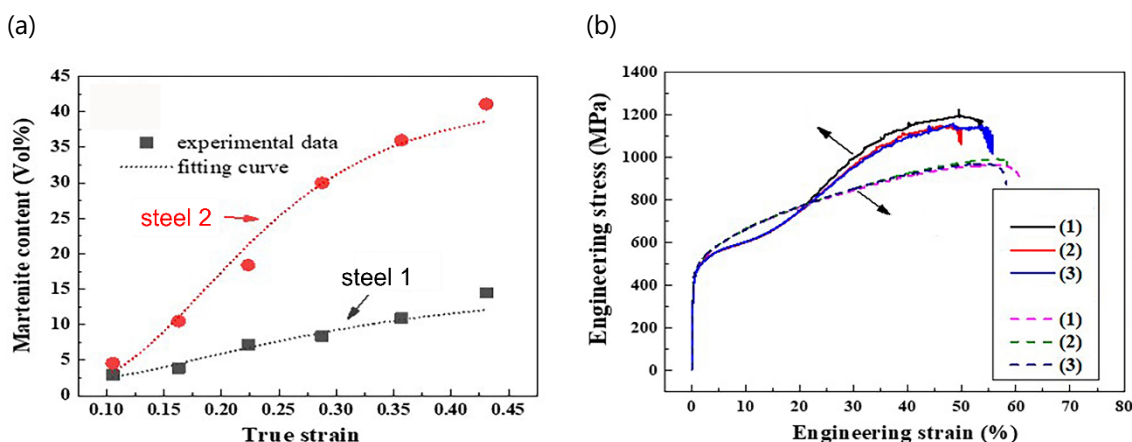


Figure 2: a) Evolution of the amount of martensite with the applied true strain; b) Engineering stress-strain curves of the steel 1 and steel 2;

- Explain the term 'stacking fault energy' (SFE)? What are the main factors affecting the SFE?
- The stacking-fault energy (SFE) is a materials property noted as γ_{SFE} in units of energy per area. Stacking faults (SFs) are modifications of the normal stacking sequence of the atomic planes in the crystal structure. The energy associated with these interruptions is the SFE. The lower the SFE, the easier the formation of SFs. SFs and SFE are responsible for the TRIP effect (hcp martensite formation) in steels. Factors influencing SFE are:
 1. Austenite grain size: smaller grains are more stable
 2. Chemical composition: Besides Mn and C changes in SFE are seen when adding Si, Cu, Cr, N
 3. Temperature: SFE is lower at lower T
 4. Strain rate: adiabatic heating increases SFE and reduces the driving force for transformation
 5. Stress state: hydrostatic compressive stresses suppress the transformation

- Which of the two steels of the Table 3 and Figure 2 has the lower SFE? Justify your answer.
- Steel 2: it has a lower C (C increases SFE) and higher amount of martensite formation (pronounced TRIP effect)

- Assign the name of the steels (steel 1 and steel 2) to the corresponding engineering stress-strain curves in Figure 2-b and justify your answer.
- Steel 2: higher strength/work hardening due to TRIP effect (pronounced martensite transformation) because of its lower SFE

2) Ni alloys (20 P)

a) Figure 3-a shows a single-crystalline (SX) turbine blade, which was made from the Ni-based superalloy CMSX-4 using the Bridgman furnace process (schematic Figure 3-b). During the casting process, the withdrawal velocity was set to 20 mm/min and the thermal gradient at the solid/liquid interface was set to 2500 K/m.

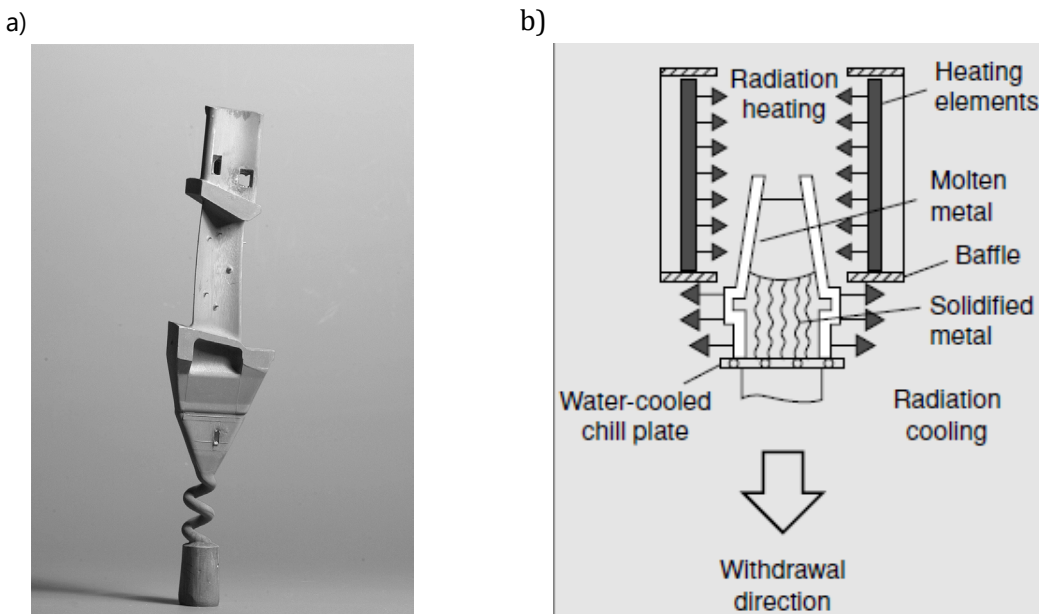


Figure 3: a) Single-crystalline turbine blade; b) schematic of the Bridgman furnace process;

- Explain the function of the 'pig-tail' in the lower part of the cast turbine blade.
- Pig tail = single crystal selector: only one grain will reach the upper part of the casting mold. Since fcc-Ni grows fastest in (100) direction, a (100) grain will be selected.
- Name and briefly explain two typical casting defects that would occur when increasing the withdrawal velocity to 40 mm/min.
 - High-angle GBs: if the withdrawal velocity is too high, the heat flow is not uniaxial anymore. The solidification front is curved and dendrites do not grow parallel anymore.
 - Globular grains: nucleation of grains ahead of solidification front and growth in all directions.

b) After casting, components fabricated from single-crystal superalloys undergo a complicated heat treatment designed to remove the microsegregation inherited from the casting process.

- Explain briefly why microsegregation occurs during casting of Ni superalloys.
 - Alloying elements have different solubility in solid and liquid phase (C_s and C_l) \rightarrow partitioning coefficient $k=C_s/C_l$
 - a. $K<1 \rightarrow$ enrichment of element x in the liquid
 - b. $K>1 \rightarrow$ enrichment of element x in solid

The element x cannot diffuse quickly enough a) from the liquid to solid or b) out of solid into liquid

- What would be the implications of not heat-treating the cast components?
 - Formation of regions with (near) eutectic compositions and low melting point in the interdendritic regions \rightarrow risk of liquation cracking upon heating
 - Non-homogeneous element distribution and variation of physical and mechanical properties in the volume

c) Creep samples from the single-crystal superalloys TMS-75 and TMS-82+ alloys were cast such that the compositions of the γ and γ' -Ni₃Al phases were on a common tie-line, so that the phase compositions remain invariant. The compositions of the two alloys (in wt.%) are given in *Table 4*. *Figure 4* shows the creep rupture life of the two alloys as a function of the fraction of the γ' phase present at 900°C and at 1100°C.

Table 4: Chemical compositions of TMS-82+ and TMS-75 (in wt.-%);

| Alloy | Co | Cr | Mo | W | Al | Ti | Ta | Hf | Re | Ni |
|---------|------|-----|-----|-----|-----|-----|-----|-----|-----|------|
| TMS-82+ | 7.8 | 4.9 | 1.9 | 8.7 | 5.3 | 0.5 | 6.0 | 0.1 | 2.4 | Bal. |
| TMS-75 | 12.0 | 3.0 | 2.0 | 6.0 | 6.0 | - | 6.0 | 0.1 | 5 | Bal. |

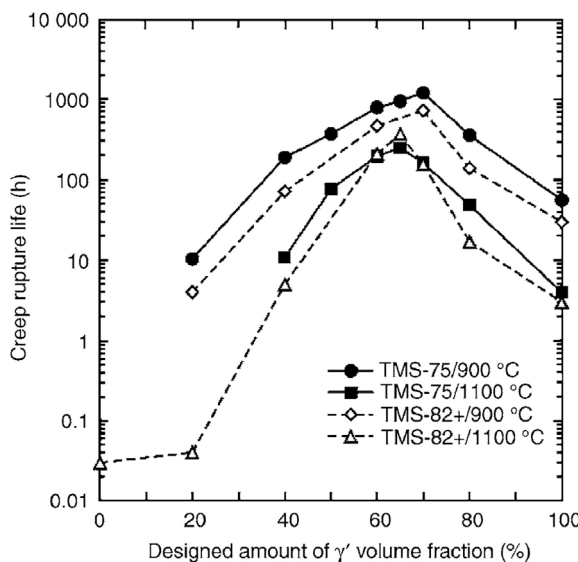


Figure 4: Creep rupture life of TMS-75 and TMS-82+ as a function of the fraction of the γ' phase ($\sigma = 392 \text{ MPa} @ T = 900^\circ\text{C}$, $\sigma = 137 \text{ MPa} @ T = 1100^\circ\text{C}$);

- Explain the general shape of the curves, i.e. the first increasing and then again decreasing creep rupture life with increasing γ' phase fraction. Why is the maximum creep resistance not imparted at a 50% fraction of γ' phase?
 - Increasing amount of γ' \rightarrow increasing particle strengthening effect
 - Beyond 60 vol% γ -channels (to which dislocation movement is constrained) become disconnected and γ' regions are predominant (creep behavior of γ' intrinsically lower than γ)
- Explain the in general higher creep rupture life of the TMS-75 alloy at γ' phase fractions below 60 vol%.

TMS-75: higher amount of mainly Co+Re

Co \rightarrow reduces SFE + solid solution strengthening

Re \rightarrow pronounced solid solution strengthener + reduction of γ'/γ -misfit \rightarrow delayed coarsening of γ'

d) Figure 5 shows the binary Ni-Al phase diagram.

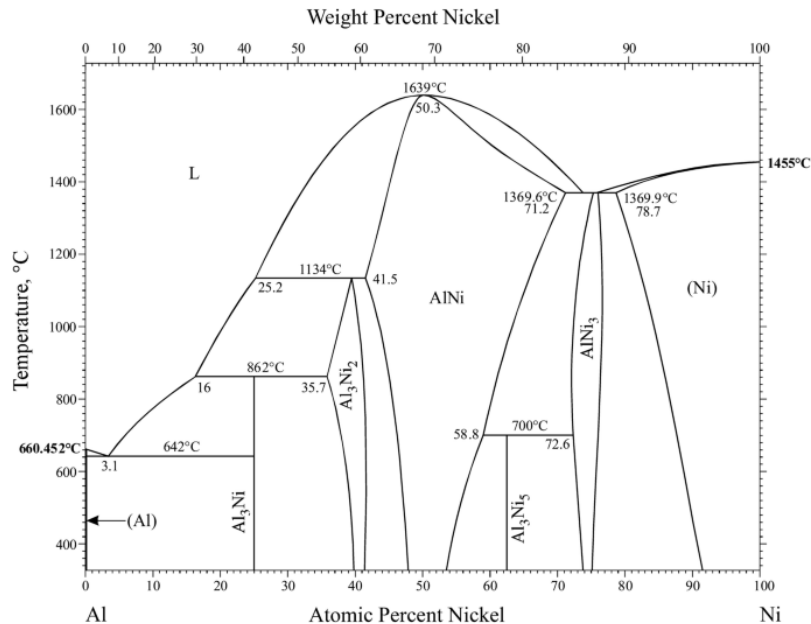


Figure 5: Binary Ni-Al diagram;

- Give two reasons why alloys with a composition of approximately 50 at.% Ni and 50 at.% Al are of interest as a replacement for Ni superalloys for high-temperature applications such as turbine blades. (2P)

- Lower density
- Higher amount of Al and thus formation of dense Al_2O_3 layer C → protection against HT corrosion
- Higher melting point than Ni and Ni-alloys

- Is the phase NiAl a Laves phase? Justify your answer. (2P)

- It is not a Laves-phase
- Laves phases are of type A_2B or AB_2
- NiAl is not

- Explain why pure NiAl exhibits a poor ductility and, as a result, a high notch sensitivity at temperatures below 650°C. (2P)
 - It is a B2 superstructure
 - High Peierls stress
 - Availability of only 3 independent slip systems
- As a result of this low ductility, shape forming of NiAl using e.g. milling or turning is extremely challenging. Name and briefly explain an alternative method that could be used to fabricate parts with more intricate geometries such as turbine blades (2P)
 - Powder metallurgy could be an alternative:
 - Fabrication of powder via e.g. EIGA
 - Shape forming
 - Sintering

3) Al and Mg alloys (16P)

a) You have been given two alloys with the following designations: AA2024 (T6) and AZ31 (T4). Based on these information, please name:

- The category of alloys these materials belong to (2P)

- AA2024 is an aluminium alloy
 - AZ31 is a magnesium alloy

- The main alloying elements and their impact (2P)

- For AA2024 : Cu and Mn offers solid solution and precipitation hardening
 - For AZ31: Al and Zn (both suitable for solid solution and precipitation hardening) and Zn also improves the oxidation resistance

- The thermal treatment these alloys have been subjected to (2P)

- For AA2024 T6: solid solution treatment and artificial ageing
 - For AZ31 T4: solid solution treatment and natural ageing

b) You have been given the responsibility for the heat treatment of a AA6063 aluminium alloy containing 0.9 wt% Mg, 0.6 wt.% Si and minor amounts of Zn and Ti.

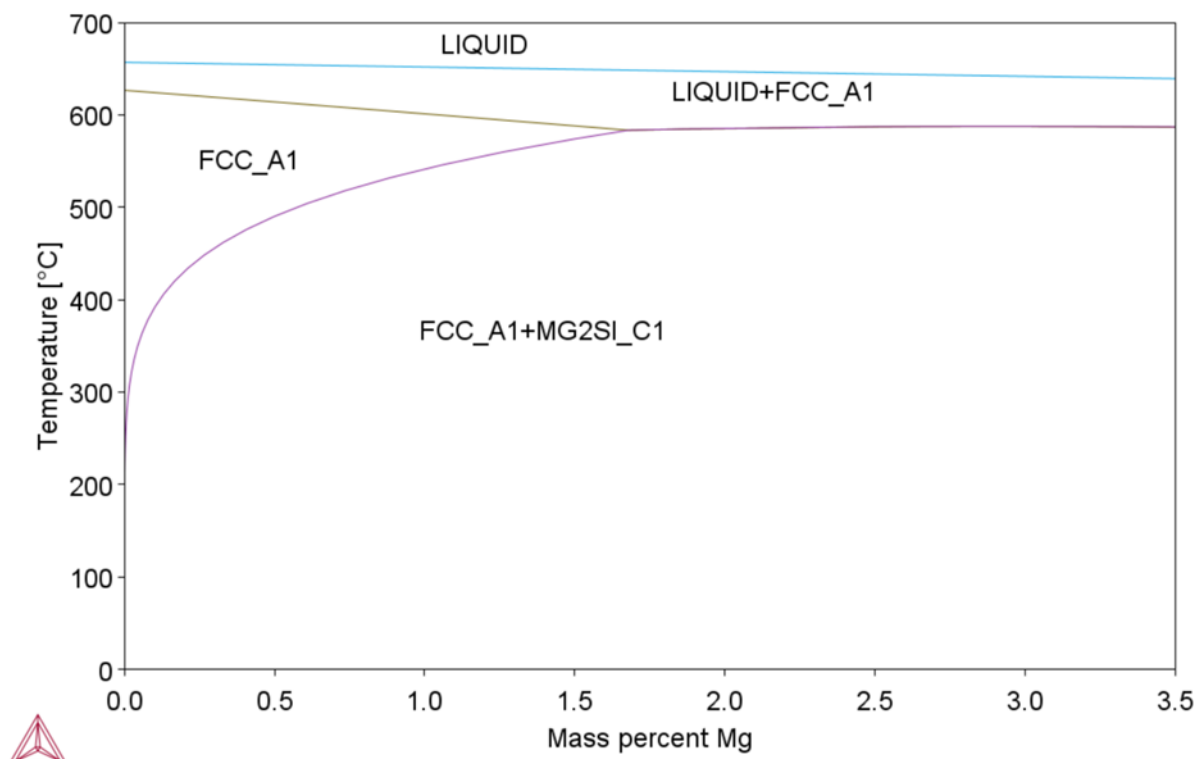


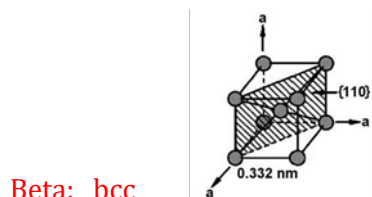
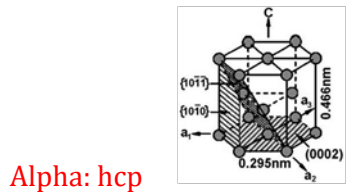
Figure 1: Quasi-binary Al0.6Si – Mg phase diagram

- In figure 1, the calculated Al-rich corner of the binary section of the Al-Mg-Si phase diagram at a fixed amount of Si of 0.6 wt.% is given. The phase diagram includes the liquid, the aluminium matrix (FCC) and the precipitation phase (Mg_2Si). Define the phase-fields on the given diagram.
- Propose a full step heat treatment in order to achieve maximum precipitation hardening (i.e. peak ageing), through the dispersion of Mg_2Si precipitates, considering that the as-received material has been subjected to extrusion.
 - Solution treatment to 550 °C for 20 h to homogenize the microstructure
 - Quenching in water to keep a supersaturated solid solution
 - Artificial isothermal ageing on 180 °C for 10h
- You decide to increase the selected temperature for the ageing treatment by 50 °C. Explain qualitatively what impact this temperature increase has on the average radius of the precipitates, their number density and the overall strength and hardness of the material, if you keep the duration of the treatment constant?
 - Average radius of precipitates ↑
 - Number density ↓
 - Overall strength and hardness ↓

- You leave a batch of solutionized and quenched samples in the laboratory (i.e. at room temperature) for 3 months. Then you measured the hardness of the samples and you figured out that there was a slight increase in comparison with the value you measured 3 months ago. Give an explanation for this hardness increase.
- Natural ageing resulted in the formation of early stage precipitates that increased the strength and hardness of the material

4) Ti Alloys

- a) In Ti alloys the addition of α stabilizers increases the α/β transformation temperature, whereas the addition of β stabilizers decreases the α/β transformation temperature.
- What are the lattice structures (names and sketches) of the α phase and of the β phase?



- Figure 7 shows schematically the influence of α and β stabilizers on the phase fields in Ti alloys. Complete the graphs with two examples for α stabilizing and two examples for β stabilizing elements in Ti alloys.

Al, Sn, Zr, O, N, C

V, Fe, Nb, Cr, Cu, Mo, Ta

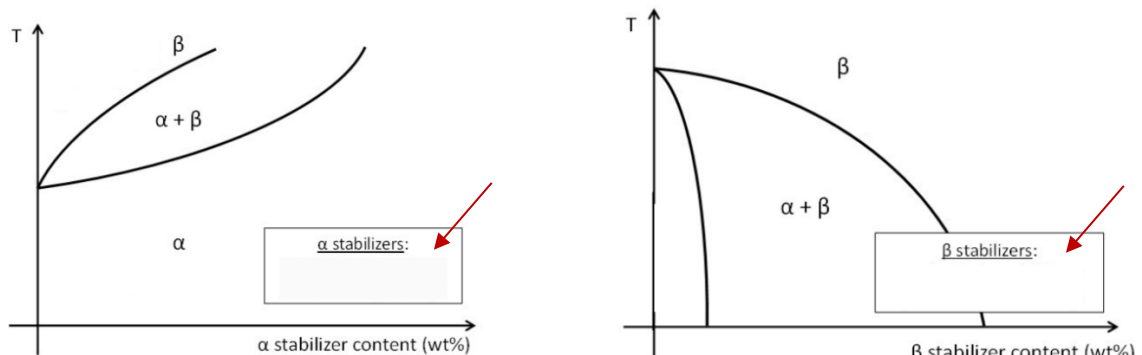


Figure 6: Influence of α and β stabilizers on the phase fields in Ti alloys;

- Based on their alloying elements (α stabilizers and β stabilizers), Ti alloys are classified as α -alloys, $\alpha + \beta$ alloys and β -alloys. Complete Table 5 defining to which class the following alloys belong to (compositions given in wt. %).

Table 5: Names and compositions (given in wt. %) of different Ti alloys;

| Alloy class | Grade | Al | Sn | Zr | Mo | Ta | Nb | Fe | O |
|----------------|---------------------|----|-----|----|----|-----|-----|------|-----|
| α | Ti-5Al-2.5Sn | 5 | 2.5 | -- | -- | -- | -- | -- | 0.2 |
| α | Ti-6Al-2Sn-4Zr | 6 | 2 | 4 | -- | -- | -- | -- | 0.2 |
| β | Ti-29Nb-13Ta | 29 | -- | -- | -- | 13 | -- | 0.03 | 0.4 |
| $\alpha+\beta$ | Ti-6Al-7Nb | 6 | -- | -- | -- | 0.2 | 7 | -- | 0.2 |
| β | Ti-15Mo-2.7Nb-0.2Si | -- | -- | -- | 15 | -- | 2.7 | 0.1 | 0.1 |
| $\alpha+\beta$ | Ti-7Al-4Mo | 7 | -- | -- | 4 | -- | -- | -- | 0.1 |

b) The compressor blades of an aero-engine are fabricated from the alloy Ti-6Al-4V. The compressor blades, after being manufactured by forging, show a bimodal microstructure that consist partly of equiaxed (primary) α in a lamellar $\alpha+\beta$ matrix. Once fabricated, the blades are welded using laser beam welding (LBW). Figure 8-a shows the geometry of the welding zone after the process. During LBW, the welded material experiences a particular thermal history, which affects the microstructure of the fabricated blades. The temperature in the weld pool was measure remotely at the position indicated by a red cross in Figure 8-a). Figure 8-b) shows the evolution of the temperature recorded by the thermocouple during the laser beam welding of the parts (red curve).

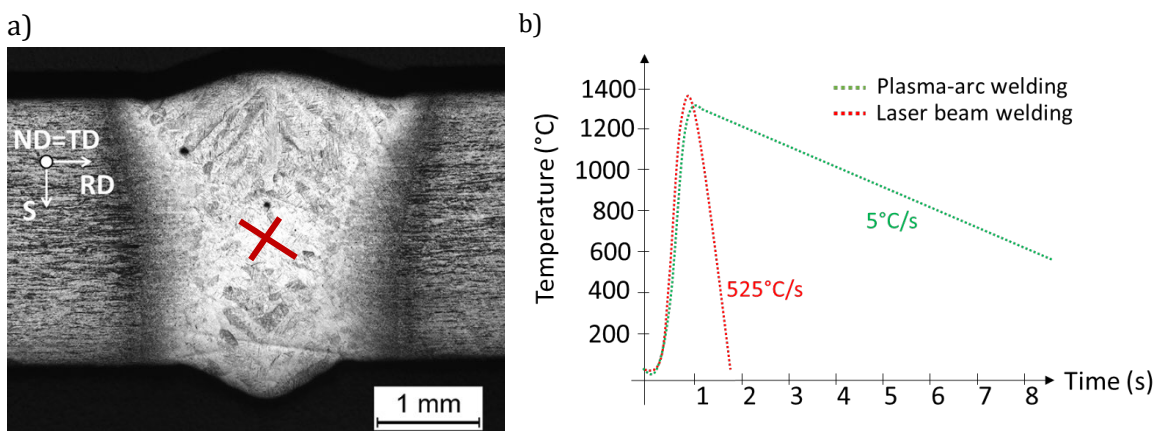
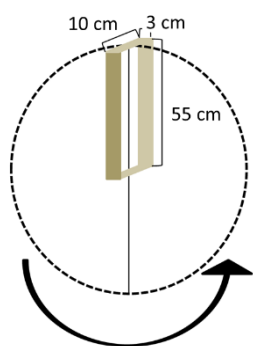


Figure 7: a) Temperature evolution measured by thermocouple at the center of the weld during laser beam welding (red curve) and during plasma-arc welding (green curve); b) geometry of the welding zone;

- Which type of microstructure do you expect to form at the center of the weld after laser beam welding? (Phase or phases, grain size)
 - Martensite α' , lamellar, very fine due to fast cooling rate

- How does the microstructure of the welding zone change if the same blades are welded by plasma-arc welding? (Consider the thermal history experienced by the welded material reported in Figure 8-a)
- Lamellae of α in a β matrix due to lower cooling rate
- c) The blades have a density of 4.4 g/cm³. The blade dimensions are 55 x 10 x 3 cm³ and rotate with an angular velocity (ω) of 6275 rpm (Figure 9). The S-N curves have been determined using rotating loading and were designed in a way to simulate as closely as possible the service condition of the blades. (NB: considering a point mass located at the extremity of the blade, the $F_{centr} = \frac{m*v^2}{r}$, where v is the velocity, m the mass of the blade and r is the radius of the circumference)

a)



b)

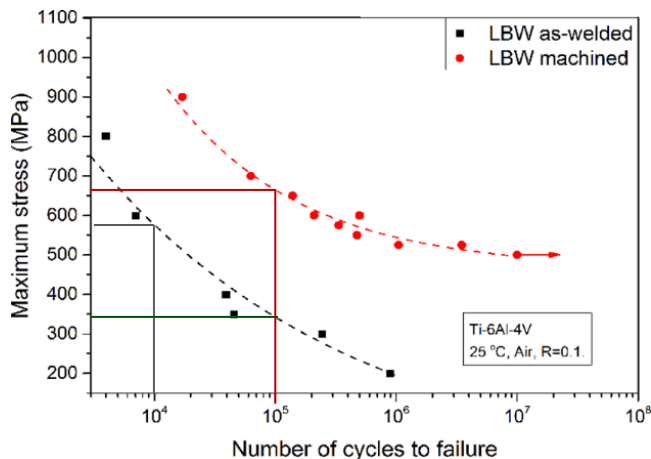


Figure 8: a) Blade dimensions and trajectory of the blade during rotation; b) S-N curves of Ti-6Al-4V samples subjected to rotating loading; both samples were laser beam welded. One sample (red curve) was machined after welding;

- Based on the S-N curves of the laser beam welded sample (no machined) in Figure 9-b, determine after how many cycles the welded blade will break.
- $F=1724 \text{ kN}$, $\sigma=575 \text{ MPa}$ from the graph $N=10000$ cycles
- Why does the fatigue behavior of the blades improve after machining?
- Reduction of notches, sharp edges and surface roughness → no stress concentration

- Determine which speed could be used in order to achieve a number of cycles of 100000 using the laser beam welded blade (no machined), using the S-N curve reported in Figure 9-b.
 - $\sigma=340 \text{ MPa}$, $F= 1020000 \text{ N}$, Speed=4826 rpm
- Determine which speed could be used in order to achieve a number of cycles of 100000 using the laser beam welded and machined blade, using the S-N curve is reported in Figure 9-b. The dimensions of the blade are the same as the ones shown in Figure 9-a.
 - $\sigma=660 \text{ MPa}$, $F= 1980000 \text{ N}$, Speed=6724 rpm

